Ab initio study of the factors affecting the ground state of rare-earth nickelates

Sergey Prosandeev, L. Bellaiche, and Jorge Íñiguez

Phys. Rev. B **85**, 214431 — Published 26 June 2012

DOI: 10.1103/PhysRevB.85.214431

Ab initio study of the factors affecting the ground state of rare-earth nickelates

Sergey Prosandeev,[1] L. Bellaiche,[1] and Jorge Íñiguez[2]
[1] *Physics Department and Institute for Nanoscience and Engineering, University of Arkansas, Fayetteville, Arkansas 72701, USA*
[2] *Institut de Ciència de Materials de Barcelona (ICMAB-CSIC), Campus UAB, 08193 Bellaterra, Spain*

We have used first-principles methods to investigate the factors that control the ground state of rare-earth nickelates, studying in detail the case of $NdNiO_3$. Our results suggest a complex phase diagram, with the bulk compounds standing on the edge of various instabilities that can be triggered by both electronic (e.g., changes in the Coulomb repulsion) and structural (e.g., epitaxial mismatch) means. In particular, we reveal that several phase transitions can be induced by epitaxial strain in thin films, and predict that a continuous transformation between insulating spin-density-wave- and metallic spin-spiral-like solutions occurs at moderate values of the in-plane mismatch. Our results provide a coherent picture of structural and electronic effects in nickelates, and have implications for current experimental and theoretical work on these compounds.

PACS numbers: 71.30.+h, 75.30.-m, 71.15.Mb

I. INTRODUCTION

Rare-earth nickelates $R\mathrm{NiO}_3$ (where R = Y, Nd, Pr, La, etc.) display metal-insulator and complex magnetic and charge-ordering transitions that can be controlled by properly choosing the R cation.[1] Thanks to the development of deposition techniques, nickelates can now be grown as high-quality ultra-thin films or in complex heterostructures. This is leading to a torrent of outstanding findings – ranging from size-[2] and dimensionality-[3] driven metal-insulator transitions (MITs) to exotic interfacial effects[4] –, and nickelates are quickly becoming a major field of research in the functional-oxides community. The physical origin of such striking effects is still debated even for the simplest (bulk) cases, and different scenarios have been proposed invoking various driving forces for the transformations.[5,6]

Here we report on a first-principles investigation of a relatively simple compound, pure $NdNiO_3$ (NNO), that we find to be in many ways representative of this family of nickel oxides. Our results render an intricate phase diagram with the bulk material standing on the edge of several instabilities, and show how electronic and structural factors – which we simulate by a varying Hubbard-U and thin-film epitaxial conditions, respectively – can induce profound changes in its ground state. In particular, our calculations reveal a complex transition sequence as a function of epitaxial strain, and set the basis for a detailed understanding of these materials.

II. METHODS

For the simulations we used the Generalized Gradient Approximation to Density Functional Theory (DFT) – more precisely, the so-called "PBE" scheme proposed by Perdew *et al.*[7]) – as implemented in the VASP package.[8] We used the "projector augmented wave" method to represent the ionic cores,[8,9] solving for the following electrons: Ni's $3p$, $3d$, and $4s$; Nd's $5s$, $5p$, and $6s$ (Nd's potential was generated by assuming a +3 ionization state and leaving three $4f$ electrons frozen in the core); and O's $2s$ and $2p$. Wave functions were represented in a plane-wave basis truncated at 500 eV, and a $2\times4\times8$ Γ-centered k-point grid was used for integrations within the Brillouin zone (BZ) corresponding to the 80-atom cell of Fig. 1. The calculation conditions were checked to render converged results.

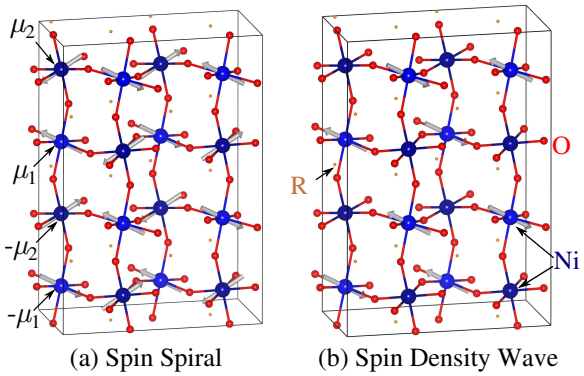

FIG. 1. (Color online). 80-atom supercell used in the simulations. The spin arrangements that we call spin-spiral [SS, panel (a)] and spin-density-wave [SDW, panel (b)] are sketched. In panel (a) we indicate the Ni magnetic moments (μ_1 and μ_2) discussed in the text and from which all others can be obtained. These SS and SDW arrangements are ideal ones, the SS being characterized by $\mu_1 \approx \mu_2$ and the SDW by $\mu_2 = 0$. The spin order in panel (a) is of the type usually denoted by $\uparrow\uparrow\downarrow\downarrow$, alluding to the sequence that occurs along any of the principal directions of the perovskite structure.

It is worth noting a couple of additional points regarding our simulations. First, we used a "Hubbard-U" correction to DFT[10] to evaluate the effect that a varying Coulomb repulsion has on the ground state of the bulk materials. Note that choosing a sound value of U to treat nickelates is not trivial, and arguments for using both large[11] and small[5] corrections have been given. Thus, to

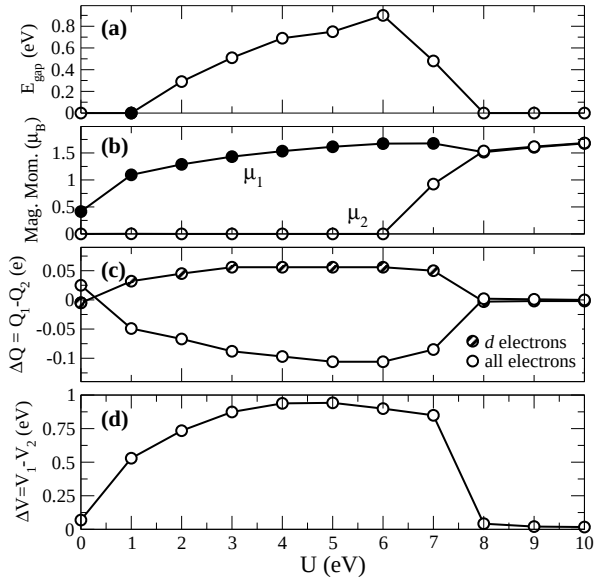

FIG. 2. (Color online). U-dependence of key electronic parameters for bulk NNO: (a) Band gap, where filled circles indicate that the zero-gap result is a marginal one (i.e., the density of states has a minimum at the Fermi energy). (b) Magnetic moments as defined in Fig. 1(a). (c) Difference ΔQ in the number of electrons around the two types of Ni cations. We show both the difference in the total number of electrons as well as the difference in electrons with $3d$ character. Essentially, the number of electrons associated to an atom is estimated by projecting the occupied electronic manifold onto localized atom-centered orbitals with specific angular momentum. (d) Difference ΔV in the electrostatic potentials experienced by the two types of Ni cations.

investigate the effect of the epitaxial strain in nickelate films, we performed all our calculations for two choices of U: 7 eV (i.e., the relatively large value most frequently adopted in the literature) and 2 eV.

Second, we worked with the 80-atom cell sketched in Fig. 1, which is essentially given by the lattice vectors $\boldsymbol{a} = 2\boldsymbol{a}_\mathrm{p} - 2\boldsymbol{b}_\mathrm{p}$, $\boldsymbol{b} = \boldsymbol{a}_\mathrm{p} + \boldsymbol{b}_\mathrm{p}$, and $\boldsymbol{c} = 4\boldsymbol{c}_\mathrm{p}$, where $\boldsymbol{a}_\mathrm{p}$, $\boldsymbol{b}_\mathrm{p}$, and $\boldsymbol{c}_\mathrm{p}$ define the elementary 5-atom perovskite cell. Our 80-atom cell is compatible with the monoclinic ($P2_1/c$) phase observed in the bulk materials at low temperatures,[12,13] which can be viewed as a distortion of an orthorhombic ($Pnma$) structure caused by the splitting of the Ni cations in two rocksalt-ordered sublattices. Our cell is also compatible with the various magnetic orders proposed to occur in these materials, as e.g. the spin-spiral (SS) depicted in Fig. 1(a) or the spin-density wave (SDW) in Fig. 1(b). As a function of epitaxial strain, we relaxed the atomic structure by (1) using a distorted $Pnma$ configuration (with all symmetries broken) as starting point and (2) imposing the constraint that the in-plane lattice vectors $\boldsymbol{a}$ and $\boldsymbol{b}$ match those of a (001)-oriented cubic substrate with lattice constant a^sub. By proceeding in this way, we effectively restricted ourselves to the consideration of phases that can be obtained as a relatively small distortion of the bulk structures; we did not attempt a more careful search for alternative phases that might be stabilized at large enough values of the epitaxial mismatch. Finally, we considered several magnetic configurations with essentially zero net magnetization; here we only report the lowest-energy states obtained.[14] Most of our simulations were done within the usual approximation of scalar magnetism; in selected cases, non-collinear spin arrangements and spin-orbit effects were considered to better characterize the ground state.

III. RESULTS AND DISCUSSION

A. U-dependence of bulk ground state

Figures 2–4 show the U-dependence of the various physical parameters characterizing the ground state of bulk NNO. Three regions are readily identified: (1) For $U > 8$ eV, we obtain metallic solutions in which all Ni's present localized magnetic moments of about 1.5 Bohr magneton (i.e., $\mu_1 \approx \mu_2 \approx 1.5\ \mu_\mathrm{B}$), and the spins arrange themselves in a SS as the one in Fig. 1(a). (2) For $U < 6$ eV, we obtain insulating solutions whose band gap (E_gap) closes continuously as U decreases, becoming zero at $U \approx 1$ eV. As regards the magnetic configuration, its most significant feature is that we have two distinct Ni sublattices: one with non-zero magnetic moments ($\mu_1 \neq 0$) whose magnitude varies continuously with U, and a second one in which the Ni ions present no localized moment ($\mu_2 = 0$); we can describe the resulting configuration as a SDW [Fig. 1(b)]. The splitting in two Ni sublattices is also evident in the charge disproportionation $\Delta Q \neq 0$ [Fig. 2(c), see discussion below] and in the relatively large difference (of as much as 1 eV) in the average electrostatic potential experienced by the two types of Ni cations [Fig. 2(d)]. Note that this large potential modulation will have a considerable impact in NNO's electronic conductivity, and should be taken into account when developing models for this compound. (3) Finally, for intermediate values of U (6 eV $< U <$ 8 eV), we obtain solutions that we call SS+SDW and which can be viewed as an interpolation between the previous two cases, i.e., as U increases the magnetic structure transforms continuously into a perfect SS and the band gap closes.

For all cases investigated, we find that NNO's structure is basically characterized by the well-known tilting of the O_6 octahedra and anti-polar displacements of the Nd cations, as shown in Figs. 3(a) and 3(b), respectively. However, the structural distortions found to be most directly linked to the observed electronic transformations are the following: (1) The *breathing*-like distortions of the oxygen octahedra (u^br) depicted in the inset of Fig. 3(c). These modes result in two rocksalt-ordered Ni sublattices, with the corresponding O_6 groups being, respectively, expanded and contracted. As regards the average Ni–O distances we have $\bar{d}_1^\mathrm{NiO} > \bar{d}_2^\mathrm{NiO}$, with $\bar{d}_1^\mathrm{NiO} \approx 2.01$ Å and $\bar{d}_2^\mathrm{NiO} \approx 1.90$ Å obtained for $U = 7$ eV.

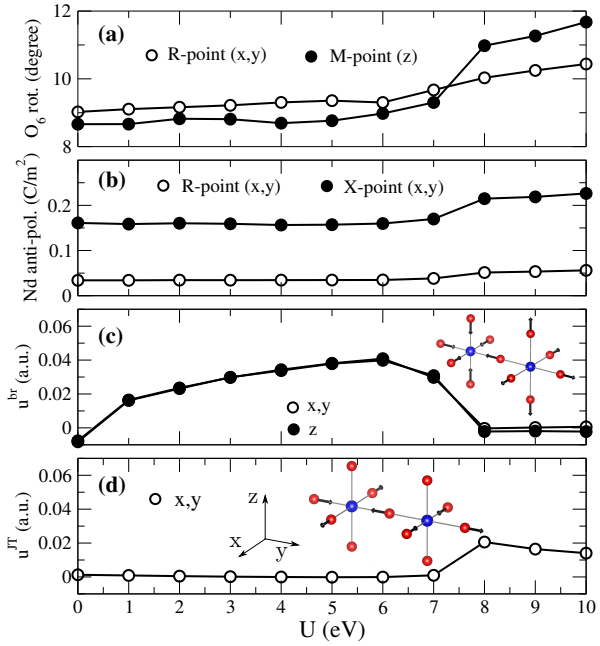

FIG. 3. (Color online). U-dependence of key structural parameters for bulk NNO: (a) Anti-phase and in-phase rotations of the O_6 octahedra. The anti-phase rotations are about the x and y pseudo-cubic directions of the perovskite structure [given, respectively, by the $\boldsymbol{a}_{\rm p}$ and $\boldsymbol{b}_{\rm p}$ described in the text, and sketched in the inset of panel (d)] and are associated with the R q-point of the Brillouin zone corresponding to the 5-atom elemental perovskite cell; the in-phase rotations are about the z pseudo-cubic axis (given by the $\boldsymbol{c}_{\rm p}$ vector described in the text) and associated with the M q-point. (b) Anti-polar displacements of the Nd sublattice, along the x and y pseudo-cubic directions and associated to the R and X q-points. To give the distortion in units of polarization, we multiply its amplitude by the nominal +3 charge of the Nd cations and divide by the cell volume; we thus obtain a rough estimate of the magnitude of the local dipoles involved in the anti-polar pattern. (c) Isotropic-breathing distortion $u^{\rm br}$ corresponding to the atomic displacement pattern shown in the inset. (d) Jahn-Teller-like distortion $u^{\rm JT}$ sketched in the inset. Note that the x, y, and z components of the various distortions shown are related in some cases.

(2) The Jahn-Teller (JT) stretching distortion of the O_6 octahedra ($u^{\rm JT}$) depicted in the inset of Fig. 3(d).[15] Note that the magnitude of these modes correlates strongly with the computed magnetic moments and band gaps; more precisely, the breathing distortions are important for $U \leq 7$ eV, and almost disappear for $U \geq 8$ eV as the JT modes become significant.

Our results for $U \lesssim 8$ eV are consistent with the $P2_1/c$ experimental ground state of these nickelates.[16] More precisely, García-Muñoz *et al.* reported $\bar{d}_1^{\rm NiO} = 1.984$ Å and $\bar{d}_2^{\rm NiO} = 1.910$ Å for NNO,[13] in good agreement with our results mentioned above. Additionally, values of $\mu_1 \approx 1.5$ $\mu_{\rm B}$ and $\mu_2 \approx 0.65$ $\mu_{\rm B}$ have been reported for related compounds $YNiO_3$[17] and $HoNiO_3$,[18] which are consistent with our results for bulk NNO obtained using

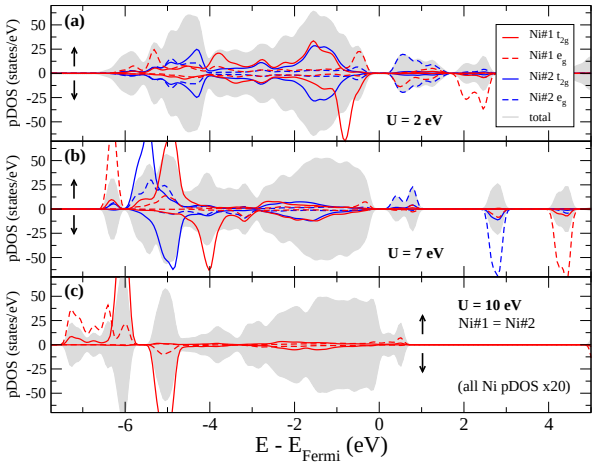

FIG. 4. (Color online). Representative results for the electronic partial density of states (DOS) close to the Fermi energy, for bulk $NdNiO_3$ and various U values. Note that the DOS associated with individual Ni atoms is scaled for clarity.

$U = 7$ eV [see Fig. 2(b)]. We also performed simulations allowing for non-collinear magnetism – which lifts the $P2_1/c$ symmetry–, and confirmed that our lowest-energy solution for $U = 7$ eV is the multiferroic "N state" discussed by Giovannetti *et al.*[11]

The above mentioned experimental results are the basis from which a charge order of the Ni atoms is usually inferred.[12,13] More precisely, the charge disproportionation δ is estimated to be about 0.25 e in NNO,[13] where e is the elemental charge; this would correspond to a difference $\Delta Q = Q_1 - Q_2 = 2\delta \approx 0.50$ e between the two Ni sublattices defined in Fig. 1. This interpretation of the experiments relies on the so-called *bond-valence model*,[19] the underlying physical picture being essentially as follows: The larger NiO_6 octahedra would be associated with a larger number of $3d$ electrons at the Ni cation, whose oxidation state would be $+3-\delta$ (ideally, +2) instead of the nominal +3; such ions would be in a high-spin configuration and display a large magnetic moment (ideally, $\mu_1 = 2$ $\mu_{\rm B}$). Conversely, the small NiO_6 octahedra would contain $Ni^{+3+\delta}$ cations (ideally, Ni^{4+}); these ions would be in a low-spin configuration and display small magnetic moments (ideally, $\mu_2 = 0$).

Interestingly, while the computed magnetic moments and interatomic distances are consistent with experiments, our estimated atomic charges do not fully support the charge order inferred in the experimental works: As shown in Fig. 2(c), for $U < 8$ eV the computed atomic charges clearly correspond to two Ni sublattices (i.e., we have $\Delta Q \neq 0$), but the magnitude of the splitting ($|\Delta Q| < 0.1$ e) is about six times smaller than the values deduced from the bond-valence analysis of the experimental data.[20] Further, the *sign* of the charge disproportionation obtained from the total number of electrons around the Ni atoms is opposite to what we would expect from the above described picture; more precisely, for the total charge we obtain $\Delta Q = Q_1 - Q_2 < 0$, implying

that the Ni atoms located at the center of the larger O_6 groups have a relatively small number of electrons bound to them. On the other hand, if we compute ΔQ by restricting ourselves to the electrons with $3d$ character, the obtained splitting has the expected sign (and continues to be small). These results clearly suggest that a simple ionic picture is not appropriate to describe and understand NNO in detail, as the strong hybridization of the nickel and oxygen orbitals may lead to counterintuitive results. (Such a strong hybridization probably explains why we *count* fewer electrons for the Ni atoms located at the bigger O_6 octahedra: the longer Ni–O distances probably imply that the electrons shared by Ni and O will be relatively far from the Ni center, which will result in a smaller number of electrons assigned to such a Ni cation.) Additionally, the difficulties to reconcile our results with the usual charge-order picture may indicate a *shift* to a Ni-Ni bond-centered charge order, as suggested in Ref. 11; further investigation is needed to clarify these issues and their practical implications. In any case, in the following we will refer to the solutions with $\mu_1 \neq \mu_2$ and $\Delta Q \neq 0$ as being "charge-ordered", to comply with the generally adopted terminology.

Our solutions for $U \geq 8$ eV are qualitatively different. In this case, all the Ni atoms present large magnetic moments indicative of a high-spin state.[21] From inspection of the projected density of states (Fig. 4), we may infer an electronic configuration somewhere between $t^3_{2g\uparrow} e^2_{g\uparrow} t^2_{2g\downarrow}$ and $t^3_{2g\uparrow} e^2_{g\uparrow} t^1_{2g\downarrow}$; note that the hybridization between Ni-$3d$ and O-$2p$ orbitals is very large, which complicates a precise assignment. Such Ni species seem compatible with the observed JT distortion. Additionally, let us note that these structures display small inversion-symmetry-breaking distortions that result in a polar space group (Pc, with polar axes along the $\boldsymbol{a}$ and $\boldsymbol{c}$ lattice vectors).[22] Nevertheless, our solutions for $U \geq 8$ eV are metallic and, thus, not ferroelectric.

B. Effect of epitaxial strain

Figures 5–9 summarize our results for the effect of epitaxial strain in NNO films. Once again, three regions are identified: (1) Within a considerable range around $a^{\rm sub} \approx 3.8$ Å, and irrespective of the value of U, the ground state is essentially that of the bulk material ($P2_1/c$ space group).[23] The simulations with $U = 7$ eV render a SS+SDW solution that can be tuned continuously towards the ideal SS (SDW) configuration by increasing (decreasing) $a^{\rm sub}$. Such a tuning is most clearly reflected in μ_2's strong dependence on the epitaxial mismatch. In contrast, the simulations with $U = 2$ eV render a SDW state whose magnetic structure varies weakly with $a^{\rm sub}$. The most significant structural distortions are the breathing modes that characterize bulk NNO and correlate with the $\mu_1 \neq \mu_2$ splitting. Naturally, in this case there is a difference between the in-plane and out-of-plane breathings; the in-plane distortion is favored as

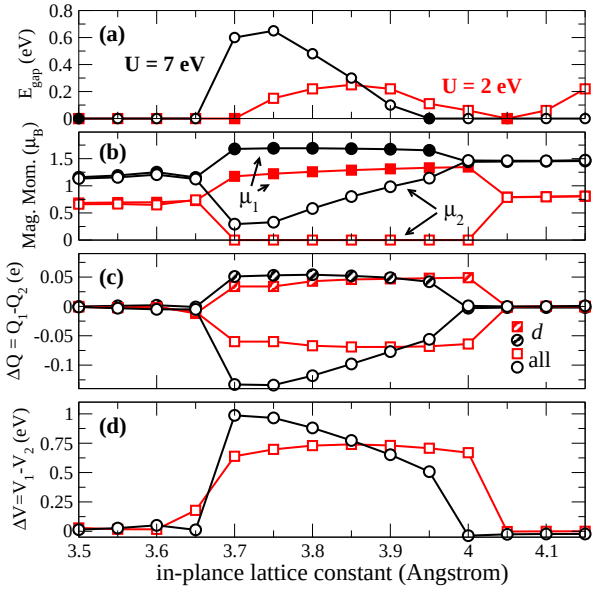

FIG. 5. (Color online). Key electronic parameters as a function of epitaxial strain, as obtained from simulations with $U = 2$ eV (red squares) and $U = 7$ eV (black circles), respectively. Details as in Fig. 2.

$a^{\rm sub}$ decreases, and the out-of-plane component presents a complicated and strongly U-dependent behavior. Finally, for both $U = 2$ eV and $U = 7$ eV, the obtained solutions are insulating throughout most of this region; the most significant changes in $E_{\rm gap}$ correspond to the $U = 7$ eV results, and clearly correlate with the magnitude of the splitting in two Ni sublattices.

(2) For large tensile strains (i.e., $a^{\rm sub} \gtrsim 4.0$ Å) we get a solution in which all Ni atoms are essentially equivalent[21] and their localized magnetic moments are arranged in a SS configuration. The disappearance of the two Ni sublattices is reflected in the dominant structural distortions, which are now of the JT type. Hence, this solution is similar to the one obtained for bulk NNO in the limit of large U; indeed, the results for $U = 7$ eV and $a^{\rm sub} \gtrsim 4.0$ Å – i.e., a metallic phase with $\mu_1 \approx \mu_2 \approx 1.5$ $\mu_{\rm B}$ – are essentially identical to our bulk results for $U \geq 8$ eV. The results for $U = 2$ eV are slightly different, as an insulating solution with $\mu_1 \approx \mu_2 \approx 0.8$ $\mu_{\rm B}$ and small $E_{\rm gap}$ is obtained in the limit of large strains. The computed partial density of states (Figs. 8 and 9) suggests that this differentiated behavior is related with a subtle U-dependence of the Ni-$3d$–O-$2p$ hybridization, which determines the nature of the levels at the Fermi energy and the existence of a gap.

(3) In the limit of strong in-plane compressions (i.e., $a^{\rm sub} \lesssim 3.65$ Å) we get solutions that somewhat resemble those obtained for large tensile strains. All Ni atoms present large magnetic moments of about 1.25 $\mu_{\rm B}$ for $U = 7$ eV and about 0.75 $\mu_{\rm B}$ for $U = 2$ eV. The solutions are metallic and a JT distortion appears. Note also that, as shown in Fig. 7, in this limit the unit cell of our

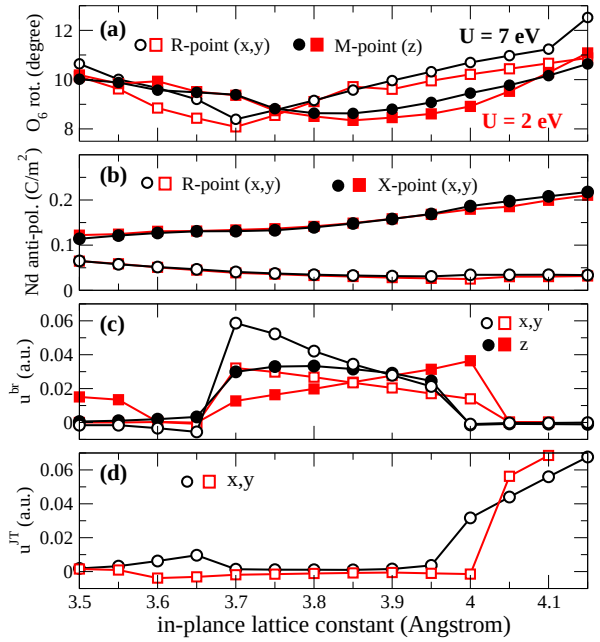

FIG. 6. (Color online). Key structural parameters as a function of epitaxial strain, as obtained from simulations with $U = 2$ eV (red squares) and $U = 7$ eV (black circles), respectively. Details as in Fig. 3.

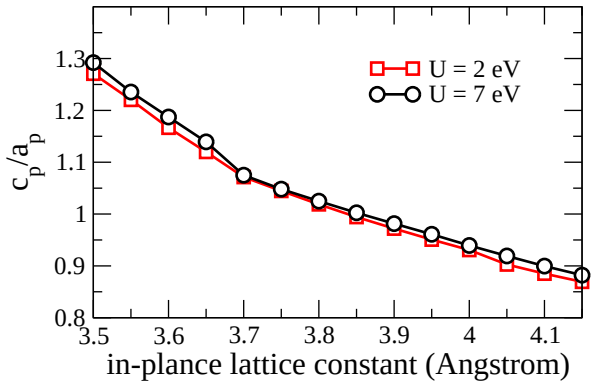

FIG. 7. (Color online). Evolution of the aspect ratio of the cell of $NdNiO_3$ films as a function of epitaxial strain, as obtained from simulations with $U = 2$ eV (red squares) and $U = 7$ eV (black circles), respectively. The reported aspect ratio (c_p/a_p) corresponds to the c_p and a_p pseudo-cubic lattice constants (see text) as deduced from our relaxed structures.

simulated NNO displays a very large aspect ratio, clearly resembling the so-called *supertetragonal* phases that can be strain-engineered in multiferroics like $BiFeO_3$.[24]

Let us remark that our results indicate that the rotations of the oxygen octahedra, around both in-plane and out-of-plane axes, are very robust in NNO. Indeed, as shown in Fig. 6(a), we do not appreciate any cancellation of specific rotation components in the considered range of epitaxial strains. Such a result may seem surprising in view of the behavior reported for other materials (e.g., $LaNiO_3$[25] and $LaAlO_3$[26]), namely, that in-plane compression favors the O_6 rotations around the out-of-plane axis and penalizes tilts around in-plane axes. Yet, let us note that the materials best investigated thus far have a rhombohedral symmetry (with a rotation pattern denoted as $a^-a^-a^-$ in Glazer's notation[27]), while here we are considering an orthorhombic compound ($a^-a^-c^+$ tilting system). Further studies will be needed to assess the generality of such a differentiated behavior between rhombohedral and orthorhombic perovskites.

Most experimental works of NNO thin films – especially for substrates in the range between $LaAlO_3$ ($a^{sub} = 3.79$ Å) and $SrTiO_3$ ($a^{sub} = 3.91$ Å) – indicate that in-plane compression favors a lower MIT temperature,[1,28–30] although the resistivity in the limit of low temperatures is not always observed to decrease accordingly.[30] In our case, for small epitaxial compressions we obtain a complex structural relaxation that leads (most clearly for $U = 7$ eV) to an enhanced charge order and increased E_{gap}; thus, our simulations suggest that in-plane compression should result in higher low-temperature resistance and, presumably, a higher MIT temperature. Hence, while it is not totally clear how to connect our results with experiments, the comparison suggests that the experimentally observed effects may not be caused by the mere epitaxial strain, which is captured exactly in our simulations. Instead, additional structural constraints that may be relevant for very thin films (e.g., O_6 rotations/distortions clamped by some substrates, effect of possible substrate twins, etc.) or extrinsic mechanisms (e.g., defects) may play an important role.

Finally, note that for $U = 2$ eV we obtain the $P2_1/c$ paraelectric space group[22] for all a^{sub} values considered; thus, the observed transitions are isosymmetric. In contrast, the calculations with $U = 7$ eV render the $P2_1/c$ phase only in the 3.70 Å $\leq a^{sub} \leq$ 3.90 Å range, as small inversion-symmetry-breaking distortions occur in all other cases. More precisely, we get the following polar solutions: $Pna2_1$ for $a^{sub} \leq 3.65$ Å (polar axis along $\boldsymbol{c}$ lattice vector), Pc for 3.95 Å $\leq a^{sub} \leq 4.00$ Å (polar axes along $\boldsymbol{a}$ and $\boldsymbol{c}$), and $Pmn2_1$ for $a^{sub} \geq 4.05$ Å (polar axis along $\boldsymbol{a}$). Nevertheless, according to our simulations all such phases are metallic and, thus, not ferroelectric.

C. Further implications of our results

Our simulations suggest that we can realistically simulate NNO by employing a Hubbard-U correction of about 7 eV, as in such conditions we get reasonable agreement with existing experimental results for the bulk material.[14] Our calculations also show that in NNO there is a close relationship between specific structural distortions, the spin state of the Ni cations, and the existence of a band gap. Such a relationship, which is consistent with the experimental observations, constitutes one of the key effects discussed in theories for the MIT in nickelates.

In such an entangled situation, an often-posed ques-

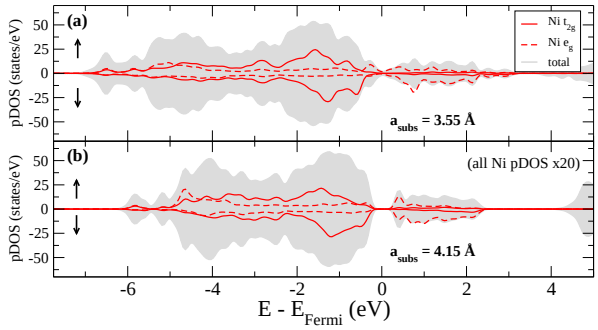

FIG. 8. (Color online). Representative results for the electronic partial density of states (DOS) close to the Fermi energy, for $NdNiO_3$ films simulated at selected a^{sub} values and with $U = 2$ eV. Note that the DOS associated with individual Ni atoms is scaled for clarity.

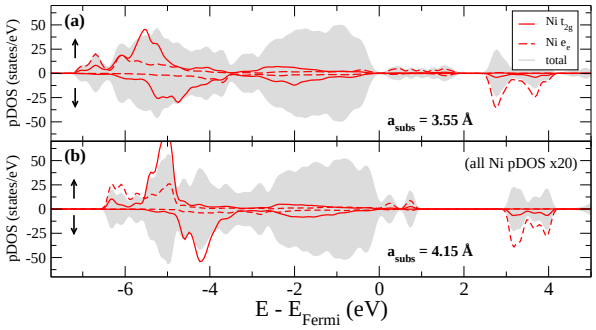

FIG. 9. (Color online). Same as Fig. 8, but for $U = 7$ eV.

tion is: What is the driving force behind the MIT in NNO and similar materials? Various electronic mechanisms have been invoked to explain the MIT, accounting for the experimentally-proposed charge order[5] and even the exotic spin order that develops in these materials.[6] Lee *et al.*[6] have also addressed the relationship between charge and spin orders. Let us briefly discuss what our simulations suggest regarding these issues.

First, we have found that bulk NNO simulated with $U = 7$ eV lies midway between two solutions – i.e., the ones we call pure SS and pure SDW, depicted in Fig. 1 – with very distinct features. In fact, NNO seems to stand on the edge of structural and electronic instabilities, and small variations in either U or the epitaxial mismatch result in profound changes in the ground state of the material. This large sensitivity suggests it may be difficult to identify a unique driving force responsible for NNO's transformations.

We have found that increasing U results in bulk states in which all Ni cations are essentially equivalent; such solutions probably correspond to the the strong-coupling limit – i.e., $U \gg t$, where t is the relevant hopping parameter – in which *all* the Ni cations tend to adopt *the same* electronic state resembling that of the isolated ion.[31] Interestingly, this U-driven (and obviously *electronic-driven*) transition between the $\mu_1 \neq \mu_2$ and $\mu_1 \approx \mu_2$ states carries with it a significant structural transformation. In particular, the breathing mode – which we identify with the charge order – disappears.

Our results indicate that similar transitions can be induced by compressing or expanding the lattice in-plane. In this case, the strong epitaxial mismatch seems to penalize the occurrence of breathing distortions of the O_6 octahedra, something that appears reasonable on geometric and steric grounds. (The breathing distortion creates relatively-large and relatively-small O_6 octahedra, which seems inadequate to accommodate either the compression or expansion of the lattice.) Then, as a result of the small-u^{br} constraint, all Ni ions present the same electronic configuration. Since the epitaxial mismatch is the control parameter for these transformations, we can interpret them as being structurally-driven. Hence, our simulations show that *both* electronic and structural mechanisms can trigger the manifold changes (structural, electronic, magnetic, band-gap) associated with transitions in NNO and related materials.

Our results show that the charge order in NNO, and the associated $\mu_1 \neq \mu_2$ splitting, strongly relies on the existence of an O_6-breathing distortion that lowers the symmetry of the material from orthorhombic ($Pnma$) to monoclinic ($P2_1/c$). Note that such a requirement goes beyond the one discussed by Lee *et al.*[6], who concluded that the orthorhombicity of the perovskite lattice is necessary for the charge order to occur. In addition, we found that the exotic $\uparrow\uparrow\downarrow\downarrow$ arrangement of the spins is still the preferred configuration among the investigated ones,[14] even in absence of charge order [i.e., for solutions with $\mu_1 \approx \mu_2$ and $u^{br} \approx 0$]; we checked that this is the case for the bulk solutions obtained with $U > 7$ eV, as well as for the films subject to large epitaxial strains simulated with $U = 7$ eV. This finding supports the claim[6] that such a spin order can exist independently from the charge order. Finally, our results indicate that small values of U tend to give a very strong charge order (with $\mu_1 \neq 0$ and $\mu_2 = 0$), while a large U of about 7 eV is needed to obtain solutions that reproduce better the experimental situation (i.e., $\mu_1 > \mu_2 > 0$). Hence, we may not fully rule out the possibility that NNO is in the weak-coupling regime,[32] as using small U values allows us to reproduce qualitatively many of the observed effects; at the same time, we obtain the best agreement with experiment for U values around 7 eV.

Finally, let us note that our preliminary results for other nickelates ($YNiO_3$, $SmNiO_3$, and $PrNiO_3$) indicate that their qualitative behavior is similar to that of NNO.[33] This suggests that the trends discussed here are essentially common to the $RNiO_3$ family, ranging from small (Y) to large (Pr) rare-earth cations.

IV. SUMMARY

In conclusion, our first-principles investigation of $NdNiO_3$ and similar materials shows that both electronic

and structural factors profoundly affect their ground state, evidencing the connections among the many (electronic, magnetic, structural) effects at play in these compounds. In particular, we predict that complex transformations – e.g., metal-insulator transitions, both drastic and continuous changes of the magnetic structure, etc. – can be induced by means of epitaxial strain in thin films. We thus hope our findings will stimulate new experimental studies of these materials, aid in the interpretation of existing and new results, and contribute to the development of realistic model theories of nickelates.

ACKNOWLEDGMENTS

J.I. thanks funding from MINECO-Spain (Grants Nos. MAT2010-18113, MAT2010-10093-E, and CSD2007-00041). S.P. and L.B. thank the financial support of ONR Grants N00014-11-1-0384 and N00014-08-1-0915, and ARO Grant W911NF-12-1-0085. They also acknowledge the NSF grants DMR-1066158 and DMR-0701558, Department of Energy, Office of Basic Energy Sciences, under contract ER-46612 for discussions with scientists sponsored by these grants. Some computations were made possible thanks to the MRI grant 0722625 from NSF, the ONR grant N00014-07-1-0825 (DURIP), and a Challenge grant from the Department of Defense. We used the software VESTA[34] to prepare some figures. Discussions with E. Canadell G. Catalán, J.L. García-Muñoz, and R. Scherwitzl are gratefully acknowledged.

[1] G. Catalan, Phase Transitions **81**, 729 (2008).
[2] R. Scherwitzl, S. Gariglio, M. Gabay, P. Zubko, M. Gibert, and J. M. Triscone, Physical Review Letters **106**, 246403 (2011).
[3] A. V. Boris, Y. Matiks, E. Benckiser, A. Frano, P. Popovich, V. Hinkov, P. Wochner, M. Castro-Colin, E. Detemple, V. K. Malik, C. Bernhard, T. Prokscha, A. Suter, Z. Salman, E. Morenzoni, G. Cristiani, H.-U. Habermeier, and B. Keimer, Science **332**, 937 (2011).
[4] M. Gibert, P. Zubko, R. Scherwitzl, J. Íñiguez, and J. M. Triscone, Nature Materials **11**, 195 (2012).
[5] I. I. Mazin, D. I. Khomskii, R. Lengsdorf, J. A. Alonso, W. G. Marshall, R. M. Ibberson, A. Podlesnyak, M. J. Martínez-Lope, and M. M. Abd-Elmeguid, Physical Review Letters **98**, 176406 (2007).
[6] S. B. Lee, R. Chen, and L. Balents, Physical Review Letters **106**, 016405 (2011).
[7] J. P. Perdew, K. Burke, and M. Ernzerhof, Physical Review Letters **77**, 3865 (1996).
[8] G. Kresse and J. Furthmüller, Physical Review B **54**, 11169 (1996); G. Kresse and D. Joubert, *ibid.* **59**, 1758 (1999).
[9] P. E. Blöchl, Physical Review B **50**, 17953 (1994).
[10] S. L. Dudarev, G. A. Botton, S. Y. Savrasov, C. J. Humphreys, and A. P. Sutton, Physical Review B **57**, 1505 (1998).
[11] G. Giovannetti, S. Kumar, D. Khomskii, S. Picozzi, and J. van den Brink, Physical Review Letters **103**, 156401 (2009).
[12] J. A. Alonso, M. J. Martínez-Lope, M. T. Casais, J. L. García-Muñoz, and M. T. Fernández-Díaz, Physical Review B **61**, 1756 (2000).
[13] J. L. García-Muñoz, M. A. G. Aranda, J. A. Alonso, and M. J. Martínez-Lope, Physical Review B **79**, 134432 (2009).
[14] We also found that a rather different solution, metallic and with a large net magnetization, is the predicted ground state of bulk NNO when using U values above 3 eV. Thus, for our chosen value of $U = 7$ eV, the calculations actually predict a ground state that is in clear disagreement with the experimental observations, and we should deem the present work as restricted to spin configurations that resemble the experimentally-observed phases, which have essentially zero remnant magnetization.
[15] The breathing mode corresponds to the R point of the Brillouin zone of the ideal 5-atom perovskite cell, while the JT distortion is associated to the M point.
[16] While RNiO$_3$ compounds with large rare-earth species (R = Pr, Nd, etc.) were initially thought to present only one type of Ni cation in their ground state [J.L. García-Muñoz, J. Rodríguez-Carvajal, P. Lacorre, and J.B. Torrance, Phys. Rev. B **46**, 4414 (1992)], recent studies of $NdNiO_3$ are consistent with the splitting in two Ni sublattices that we found in our simulations.[13] The situation of the compound with Nd thus seems similar to what is known for the materials with small rare earths[12] (R = Lu, Y, or Ho).
[17] J. A. Alonso, J. L. García-Muñoz, M. T. Fernández-Díaz, M. A. G. Aranda, M. J. Martínez-Lope, and M. T. Casais, Physical Review Letters **82**, 3871 (1999).
[18] M. T. Fernández-Díaz, J. A. Alonso, M. J. Martínez-Lope, M. T. Casais, and J. L. García-Muñoz, Physical Review B **64**, 144417 (2001).
[19] I. D. Brown, Chem. Rev. **109**, 6858 (2009).
[20] The scheme employed to estimate atomic charges tends to render values that are too small, as evidenced by the fact that the sum of the electronic charges assigned to all the atoms does not reach the total number of electrons. Further, the hybridization between Ni and O orbitals is clearly very large in these nickelates. As a result of these two factors, the estimated ionization states deviate significantly from the nominal ones that would correspond to the ionic limit. Thus, here we only report charge differences, which are of greater physical significance than the values obtained for individual atomic charges.
[21] Having $\mu_1 \approx \mu_2$ does not imply that all Ni atoms are crystallographically equivalent. In fact, for all Ni's to be equivalent, we would need to have a perfect *Pnma* symmetry, which we never observed.
[22] To determine the symmetry of our relaxed structures, we used the program FINDSYM [H.T. Stokes and D.M. Hatch (2004), http://stokes.byu.edu/isotropy.html] employing a value of 0.01 Å for the accuracy within which atomic po-

sitions and lattice vectors are known.

[23] For bulk NNO and $U = 7$ eV, we obtain a pseudo-cubic in-plane lattice constant of about 3.87 Å. Experimentally, the pseudo-cubic in-plane lattice constant of NNO is about $5.38/\sqrt{2}$ Å = 3.80 Å, as derived from the results of Ref. 13 at 50 K.

[24] H. Bea, B. Dupe, S. Fusil, R. Mattana, E. Jacquet, B. Warot-Fonrose, F. Wilhelm, A. Rogalev, S. Petit, V. Cros, A. Anane, F. Petroff, K. Bouzehouane, G. Geneste, B. Dkhil, S. Lisenkov, I. Ponomareva, L. Bellaiche, M. Bibes, and A. Barthelemy, Physical Review Letters **102**, 217603 (2009).

[25] S. J. May, J. W. Kim, J. M. Rondinelli, E. Karapetrova, N. A. Spaldin, A. Bhattacharya, and P. J. Ryan, Physical Review B **82**, 014110 (2010).

[26] A. J. Hatt and N. A. Spaldin, Physical Review B **82**, 195402 (2010).

[27] A. M. Glazer, Acta Crystallographica Section A **31**, 756 (1975).

[28] G. Catalan, R. M. Bowman, and J. M. Gregg, Physical Review B **62**, 7892 (2000).

[29] J. Liu, M. Kareev, B. Gray, J. W. Kim, P. Ryan, B. Dabrowski, J. W. Freeland, and J. Chakhalian, Applied Physics Letters **96**, 233110 (2010).

[30] R. Scherwitzl, P. Zubko, I. G. Lezama, S. Ono, A. F. Morpurgo, G. Catalan, and J. M. Triscone, Advanced Materials **22**, 5517 (2010).

[31] This would correspond to the strong-coupling limit discussed in S.B. Lee, R. Chen, and L. Balents, Phys. Rev. B **84**, 165119 (2011).

[32] Mazin *et al.*[5] studied the pressure dependence of $E_{\rm gap}$ of RNiO$_3$ compounds, concluding that small-U corrections give better agreement with experiment. Lee *et al.*[6] explained the magnetic order in NdNiO$_3$ as relying on a type of Fermi-nesting mechanism that is usually associated with weak correlations.

[33] S. Prosandeev, L. Bellaiche, and J. Íñiguez, unpublished.

[34] K. Momma and F. Izumi, Journal of Applied Crystallography **41**, 653 (2008).